

# Atomic Shuffling Dominated Mechanism for Deformation Twinning in Magnesium

B. Li\* and E. Ma

Department of Materials Science and Engineering and Center for Advanced Metallic and Ceramic Systems, Johns Hopkins University, Baltimore, Maryland 21218, USA

(Received 5 April 2009; published 17 July 2009)

Deformation twinning is often mediated by partial dislocation activities at the twin boundary. Using molecular dynamics simulations, we have uncovered a new mechanism for the most commonly observed  $\{10\bar{1}2\}\langle 10\bar{1}\bar{1}\rangle$  deformation twinning in Mg and other hexagonal close-packed metals. Here the twin growth involves no definable dislocations at the twin boundary, and the twin orientational relationship can be established by local atomic shuffling, directly constructing the twin lattice from the parent lattice.

DOI: 10.1103/PhysRevLett.103.035503

PACS numbers: 61.72.Mm, 62.20.F-

Magnesium and its alloys are currently of great interest, as their extraordinarily low densities ( $\sim 1.74 \text{ g/cm}^3$ ) are very attractive for automotive and aerospace applications. However, the plastic deformation mechanisms of Mg are not well understood. As a typical example of all hexagonal-close-packed (hcp) metals, the plastic flow in Mg involves profuse twinning activities [1–15], due to the limited number of slip systems for dislocation glide in the hcp structure. Twinning is also a major contributor to the development of texture [3–11], which greatly influences the mechanical properties. Therefore, it is very important to understand the twinning processes in Mg, for microstructural design, processing and applications.

For Mg, the most common twinning plane is the  $\{10\bar{1}2\}$  in the  $\langle 10\bar{1}\bar{1}\rangle$  direction [1,2]. This  $\{10\bar{1}2\}\langle 10\bar{1}\bar{1}\rangle$  twinning mode is also commonly seen in many other hcp metals. Such a twinning scheme cannot be accomplished by a homogeneous shear [1], and is thus very different from that in the face-centered-cubic (fcc) metals. In the higher-symmetry fcc case, the twinning plane is the close-packed  $\{111\}$ , and the twin nucleation and growth are controlled by well-defined *partial* dislocations that propagate on successive  $\{111\}$  planes [16]. In contrast, for hcp metals, twinning does not happen on the close-packed (0001) basal planes at all. It is unclear as to exactly what processes, partial dislocations or otherwise, are responsible for the deformation twinning observed.

Regarding the  $\{10\bar{1}2\}\langle 10\bar{1}\bar{1}\rangle$  twinning in Mg, previous studies have revealed that the magnitude of the shear is  $s \approx 0.129$  [17]. The  $\{10\bar{1}2\}$  interplanar spacing is  $d \approx 0.19 \text{ nm}$ . Thus the shear involved on each  $\{10\bar{1}2\}$  plane, equivalent to the Burgers vector of a hypothesized “elementary twinning dislocation”, is

$$b_T = sd \approx 0.025 \text{ nm} \quad (1)$$

This is, however, only  $\sim 1/31$  of the lattice vector in the  $\langle 10\bar{1}\bar{1}\rangle$  direction for this twinning mode. As a result, it is unlikely that there could exist such a small partial dislocation, and the growth of this twin at the twin boundary (TB) may need a “zonal dislocation” [1,17,18], defined as a

twinning dislocation with its core spreading over multiple twinning planes. So far it is unknown if any identifiable (zonal) dislocation is indeed present, or need to be involved, for the  $\{10\bar{1}2\}$  twinning.

In the following, we resolve the atomic-level mechanism of the  $\{10\bar{1}2\}\langle 10\bar{1}\bar{1}\rangle$  twinning in Mg, using molecular dynamics (MD) simulations. We demonstrate that, given the small shear [see Eq. (1)] and minor displacement (see below) required on each plane, atomic shuffling, i.e., inhomogeneous displacements of an ensemble of atoms in the layers immediately adjacent to the TB, would be all it takes to accomplish the growth of this popular twin. This scenario is different from those in metals of other types of crystal structures or in other hcp twinning systems [1,19], where the twin growth requires the action or assistance of (partial or zonal) dislocations with readily defined Burgers vectors. These latter “twinning dislocations” are known to come from many viable sources such as sessile pole dislocations, grain boundaries, and dislocation reactions.

Our modeling employs the EAM interatomic potential [20] created using the force matching method, fit to experimental as well as *ab initio* data. The potential gives a basal stacking fault energy of  $55 \text{ mJ/m}^2$ , comparable to experimental and simulated values [21]. The initial configuration of the system is shown in Fig. 1(a). Two single crystals were bonded together, in the twinning orientational relationship across the  $(10\bar{1}2)$  TB plane (edge-on from this  $[1\bar{2}10]$  viewing direction), and then fully relaxed. The alternately colored basal planes show the *ABAB...* hcp stacking sequence. The system was loaded at 10 K with a shear strain applied to the atoms on the top layer by displacing them rightward at a constant displacement rate (strain rate  $\sim 10^8/\text{s}$ ), while fixing the atoms on the bottom layer during the deformation. One million atoms were used in the simulation, in a  $40 \text{ nm} \times 40 \text{ nm} \times 15 \text{ nm}$  box, with free surfaces. Figure 1(b) is a schematic showing four  $\{10\bar{1}2\}$  layers, as examples of the non-close-packed, twinning plane. The  $d$  is  $0.19 \text{ nm}$ , significantly smaller than that of the basal plane ( $0.26 \text{ nm}$ ) and the  $\{10\bar{1}1\}$  pyramidal (also a twinning plane ( $0.24 \text{ nm}$ )). The atoms on each plane are

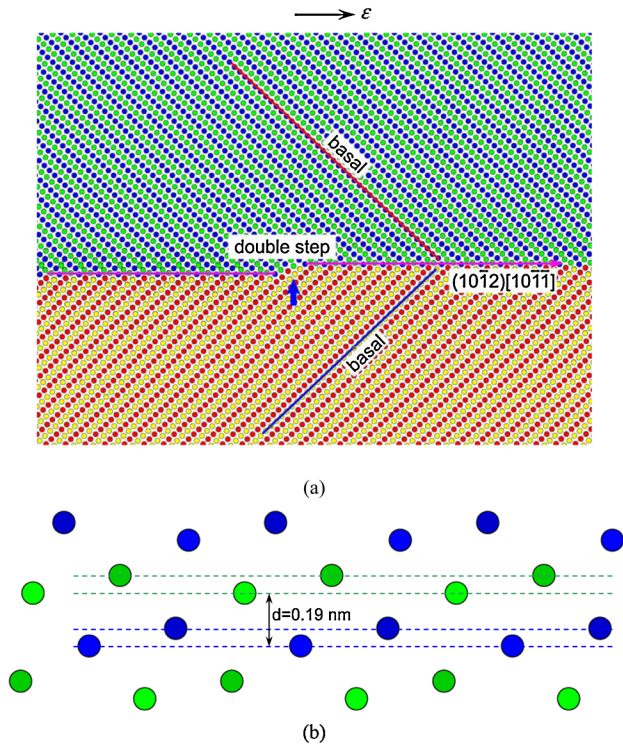


FIG. 1 (color online). (a) Projection view of a relaxed  $(10\bar{1}2)[10\bar{1}\bar{1}]$  TB (viewing direction  $[1\bar{2}10]$ ). The basal planes of the crystals on both sides of the TB are colored differently to show the  $ABAB\dots$  stacking sequence. A two-layer step (double step  $[1,17]$ ) is created to observe the mobility of such a zonal dislocation. (b) A magnified view of the “double layer” (dashed lines with the same color) structure of the  $\{10\bar{1}2\}$  twinning plane. The interplanar spacing is 0.19 nm.

actually located on two slightly separated layers. Because of this corrugated topology, the effective interplanar spacing is even smaller. Consequently, dislocation slip on this rugged plane is difficult and has never been observed.

Under the externally imposed shear strain, the TB gradually moves upward. This widening of the twin can be seen by comparing Fig. 2(a) with Fig. 1(a). The “double step”  $[1,17]$  preconstructed at the  $\{10\bar{1}2\}$  TB plane turns out to be immobile, indicating that such steps have little dislocation characteristics, and do not constitute a “zonal dislocation” that mediates TB migration. During the twin growth, a number of similar steps are formed at the TB (indicated by arrows in Fig. 2(a), to be discussed in detail elsewhere). Here we focus on how the twinning orientational relationship is established, i.e., the structural evolution or reconstruction during the twin growth. The basal plane of the twin and that of the matrix (top crystal) are each marked by a red solid line: they are seen to be nearly perpendicular to each other, as expected from the crystallographic orientational relationship of the  $\{10\bar{1}2\}\langle 10\bar{1}\bar{1}\rangle$  twinning mode. A striking feature that can be seen from the colored presentation is that, after the TB has migrated from the original position in Fig. 1(a) to that (pink line) in Fig. 2(a), the atoms in the grown twin actually have moved very little

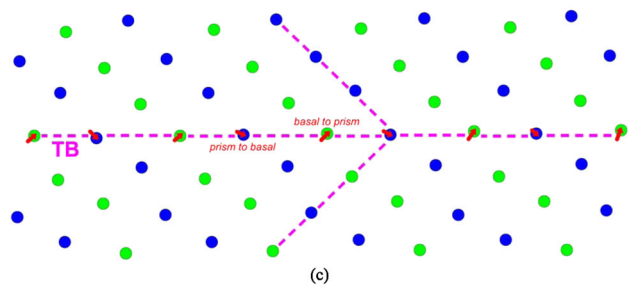
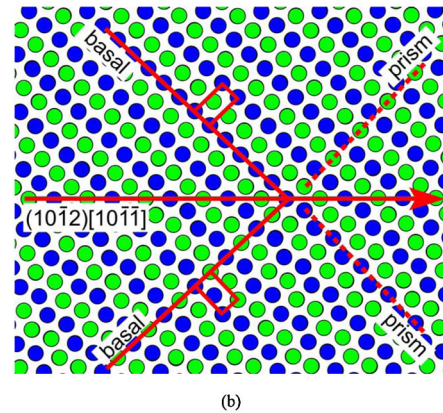
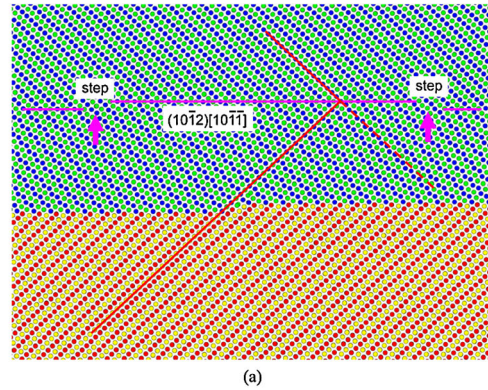


FIG. 2 (color online). (a) The twinning orientational relationship across the TB (pink line), established during twin growth. (b) A magnified view near the TB, with the red arrow indicating the twinning direction. The basic repeating unit (red box) in the matrix (top crystal above TB) is perpendicular to that in the twin. The flat basal plane in the matrix becomes the corrugated prism plane in the twin, and the corrugated prism plane in the matrix becomes the flat basal plane. (c) Shuffling displacements (2D projection) experienced by the atoms at the TB to achieve the prism-basal conversion in (b). An arrow is attached to each atom to show the displacement.

from their original positions on the parent basal planes. As an example, a dashed red line is drawn, extending the parent lattice (blue atoms on the solid line) into the twin lattice. The new positions of the atoms in the grown twin are observed to deviate from those on the original matrix lattice (dashed red line) by a very small distance. Between any two successive  $\{10\bar{1}2\}$  layers, the relative shift is much smaller than an atomic spacing. In other words, the shear displacement in the twinning direction for this twinning mode is very small indeed [see Eq. (1)].

A close-up view of the lattices near the moving TB is shown in Fig. 2(b). Comparing the lattices across the TB, the atoms on the straight basal planes in the parent lattice (top crystal), are now located on the corrugated prism planes in the twin (bottom crystal) after the TB traverses. In the meantime, the parent prism planes have now become the basal planes in the twin. In the MD simulation movie [22], the TB moves up two  $\{10\bar{1}2\}$  layers (the period of the corrugation seen in Fig. 2(b) and in the movie in [22]) at a time, with atomic shuffling to establish the twin mirror relationship. We also plot in Fig. 2(c) the displacements experienced by the atoms at the TB (see the arrow attached to each atom, marking the projection to the  $(\bar{1}210)$  plane) from their positions in the parent matrix to the positions after they join the growing twin.

There are several indications that the realization of the twinning relationship shown in Fig. 2 and in the movie [22] does not result from an identifiable zonal dislocation at the TB. First, the topological interfacial dislocations suggested for the  $\{10\bar{1}2\}$  TB in simulations of hcp crystals [23–25] were not observed here. The two-layer step shown in Fig. 1 is not mobile. Second, without such a double step [1,17], or if we start with a crystal without a preexisting TB, the twinning and lattice conversion shown above still occur (not shown). Third, while there is a net shear component in the twinning direction [to the right, see Fig. 2(c)], its magnitude is only  $\sim 0.025$  nm for each layer [also see Eq. (1)]. That of a “double-step zonal dislocation” ( $2b_T$ ) would also be as small as  $\sim 0.05$  nm. Dislocations carrying such small displacements could neither recover the lattice (a full dislocation) nor carry the lattice to a metastable energy state (a partial dislocation and a stacking fault). Fourth, as seen in Fig. 2(c), a given atom would be moving in a direction almost perpendicular to its neighbors (see Fig. 3 for the required displacements in three dimensions), such that a dislocation process would be difficult. Fifth, the small net shear appears to directly result from the collective shuffling actions themselves (see movie [22]). Sixth and finally, the magnitude of the shuffling displacement of each atom reaches  $\sim 0.09$  nm [in Figs. 2(c) and 3 below], much larger than the 0.025 nm shear in the  $\langle 10\bar{1}\bar{1} \rangle$  twinning direction. We thus believe that the mechanism for the  $\{10\bar{1}2\}\langle 10\bar{1}\bar{1} \rangle$  twinning can be best characterized as atomic shuffling dominated. While twinning in hcp is generally not accomplished by a homogeneous shear alone (as in fcc) and requires the atoms near the non-close-packed TB plane to adjust their positions [1], our example here represents an extreme case where the atomic displacements are in such different directions and magnitudes that negate any well-defined dislocation activity [1,17]. Meanwhile, the shear displacement of each  $\{10\bar{1}2\}$  layer relative to the next layer is so minor that it can be achieved simply by the net vector of all the shuffles involved. In contrast, the  $\{10\bar{1}1\}\langle 10\bar{1}\bar{2} \rangle$  twinning mode in Mg is dominated by shear in the twinning direction ( $\sim 0.15$  nm on each  $\{10\bar{1}1\}$  layer,  $\sim 0.29$  nm for the two-layer step as the zonal dislocation, with only minor local shuffling of  $\sim 0.04$  nm [19]). There, a well-

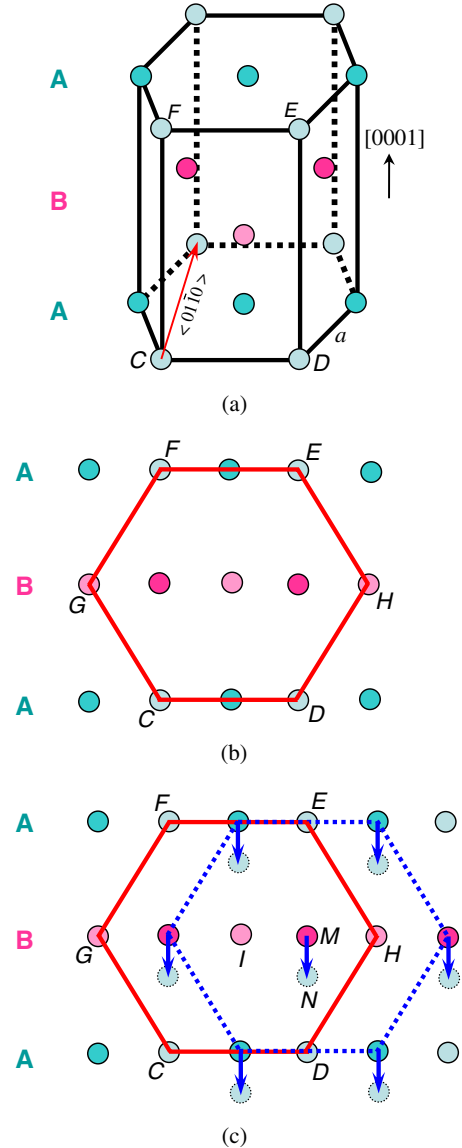


FIG. 3 (color online). (a) 3D view of the hcp Mg lattice. The colored basal planes show the normal stacking sequence  $ABAB\dots$  along the  $\langle c \rangle$  direction. (b) The projection view of the 3D lattice in the direction along  $\langle 01\bar{1}0 \rangle$ . A new basal plane can be constructed by connecting the atoms with  $\sim a$  spacing. See text for the adjustment shuffling needed. (c) To establish the correct hcp stacking sequence shuffling must also move the marked atoms by  $1/6\langle c \rangle$  ( $\sim 0.09$  nm); see arrows pointing to the final positions (dashed circles).

defined zonal dislocation is clearly involved and shown to be a form of the incomplete dislocation on the pyramidal plane in the matrix [26].

To resolve exactly what shuffling results in the conversion shown above between the basal and prism planes, we show in Fig. 3(a) a 3D view of a normal hcp lattice of Mg. The  $ABAB\dots$  basal planes are marked with different colors, and so are the atoms that lie in different prism  $\{10\bar{1}0\}$  planes. In Fig. 3(b), we take the projection view along the zone axes  $\langle 01\bar{1}0 \rangle$  (perpendicular to the  $c$  axis).

Each basal plane now becomes a row of atoms with different colors. The 2D plot immediately reveals the possibility of constructing a hexagonal, new “basal” plane from the existing lattice points, if we connect some of the atoms in the pattern shown in Fig. 3(b). The new basal plane comes from the prism planes of the original lattice and is  $90^\circ$  away from the original basal planes. This basal-prism conversion and the  $90^\circ$  orientational difference, in the absence of any actual crystal rotation, is similar to what have been revealed in Fig. 2, where the basal planes of the parent crystal and the twin are close to being perpendicular to each other.

However, the lattice reconstruction shown in Fig. 3(b) does not have the correct hcp packing, yet. Some structural deviations have to be corrected and adjusted. This is why atomic shuffling is critical to accomplish the conversion or twinning. First, the new basal plane reconstructed in Fig. 3(b) is distorted. The atoms in the middle layer (pink atoms such as *G* and *H*) do not fall exactly on the same plane formed by the other atoms (green ones, *F*, *E*, *C*, *D*) from the top and the bottom layers. The absolute deviation equals  $\sqrt{3}a/6$  ( $\sim 0.09$  nm). Therefore, atoms *G*, *I* and *H* have to move outward (in the direction perpendicular to the paper plane ( $1\bar{2}10$ )).

Second, the magnitudes of the connections *FE*, *FG*, etc., in Fig. 3(b) are nearly but not exactly equal to the lattice parameter *a*. The deviation is  $(\sqrt{\frac{\gamma^2}{4} + \frac{1}{3}} - 1)a$ , which is zero for ideal *c/a* in the hard-sphere hcp packing, and  $< 0.5\%$  for Mg, thus requiring minimal shuffling correction.

Third, to accomplish the hcp *ABAB...* stacking sequence in the direction perpendicular to the new basal plane (*A*), another basal plane (*B*) has to be reconstructed in the right position. As seen in Fig. 3(c), this requires that the atoms in the second basal (dashed blue line connections) to be projected to the center of the triangles in the first basal; examples are shown by the dashed circles such as position *N*. But this requirement is not satisfied in Fig. 3(b). Atoms such as *M* have to shuffle down to new positions like *N*, by a displacement of  $1/6[0001]$  ( $\sim 0.09$  nm) (blue arrows).

Finally, minor shuffling ( $\sim 0.02$  nm) is required to reach the correct *c/a* ratio in the twin lattice. Notably, the magnitude of all the required shuffling, with the largest displacement being  $\sim 0.09$  nm, is much smaller than any existing Burgers vectors for dislocations in Mg, such as  $\langle a \rangle$  ( $1/3\langle 2\bar{1}\bar{1}0 \rangle = 0.321$  nm),  $\langle c \rangle$  ( $[0001] = 0.52$  nm),  $\langle c + a \rangle$  ( $1/3\langle 11\bar{2}3 \rangle = 0.61$  nm), or the partial dislocations such as the one mediating  $\{10\bar{1}1\}\{10\bar{1}\bar{2}\}$  twinning ( $0.29$  nm) [19,26].

To conclude, the growth of the  $\{10\bar{1}2\}\{10\bar{1}\bar{1}\}$  deformation twin in Mg via the migration of the TB can be accomplished by atomic shuffling predominantly in the two  $\{10\bar{1}2\}$  layers of the parent lattice immediately adjacent to the TB. The resulting lattice reorientation, forming a twin with a misorientation  $\sim 90^\circ$  to the matrix, is

achieved by the conversion of the basal planes to prism planes (and vice versa). This structural reconstruction is mediated by atomic shuffling, without the action of, and need for, a well-defined dislocation. Our findings explain why the  $\{10\bar{1}2\}\{10\bar{1}\bar{1}\}$  is the most commonly observed twinning mode in Mg and other hcp metals, even though dislocation processes on this twinning plane are unknown and difficult.

This work is supported by ARMAC-RTP, DAAD19-01-2-0003 and W911NF-06-2-0006.

\*bli@jhu.edu

- [1] J. W. Christian and S. Mahajan, Prog. Mater. Sci. **39**, 1 (1995).
- [2] M. M. Avedesian and H. Baker, *Magnesium and Magnesium Alloys*, ASM Specialty Handbook (ASM International, Materials Park, Ohio, 1999).
- [3] J. Bohlen, M. R. Nurnberg, J. W. Senn, D. Letzig, and S. R. Agnew, Acta Mater. **55**, 2101 (2007).
- [4] S. R. Agnew, P. Mehrotra, T. M. Lillo, G. M. Stoica, and P. K. Liaw, Mater. Sci. Eng. A **408**, 72 (2005).
- [5] M. R. Barnett, M. D. Nave, and C. J. Bettles, Mater. Sci. Eng. A **386**, 205 (2004).
- [6] R. D. Field, K. T. Hartwig, C. T. Necher, J. F. Bingert, and S. R. Agnew, Metall. Mater. Trans. A **23**, 965 (2002).
- [7] W. J. Kim, C. W. An, Y. S. Kim, and S. I. Hong, Scr. Mater. **47**, 39 (2002).
- [8] S. R. Agnew, J. A. Horton, T. M. Lillo, and D. W. Brown, Scr. Mater. **50**, 377 (2004).
- [9] M. J. Phillipe, F. Wagner, F. E. Mellab, C. Esling, and J. Wegria, Acta Metall. Mater. **42**, 239 (1994).
- [10] M. J. Phillipe, M. Serghat, P. Van Houtte, and C. Esling, Acta Mater. **43**, 1619 (1995).
- [11] J. J. Funderberger, M. J. Phillipe, F. Wagner, and C. Esling, Acta Mater. **45**, 4041 (1997).
- [12] T. Mukai, M. Yamanoi, H. Watanabe, and K. Higashi, Scr. Mater. **45**, 89 (2001).
- [13] Y. N. Wang and J. C. Huang, Acta Mater. **55**, 897 (2007).
- [14] S. R. Agnew and J. R. Weertman, Mater. Sci. Eng. A **242**, 174 (1998).
- [15] B. Plunkett, R. A. Lebensohn, O. Cazacu, and F. Barlat, Acta Mater. **54**, 4159 (2006).
- [16] S. Mahajan and G. Y. Chin, Acta Mater. **21**, 1353 (1973).
- [17] N. Thompson and D. J. Millard, Philos. Mag. **43**, 422 (1952).
- [18] S. Vaidya and S. Mahajan, Acta Metall. **28**, 1123 (1980).
- [19] B. Li and E. Ma, Acta Mater. **57**, 1734 (2009).
- [20] X. Y. Liu, J. B. Adams, F. Erocolessi, and J. A. Moriarty, Model. Simul. Mater. Sci. Eng. **4**, 293 (1996).
- [21] R. L. Fleischer, Scr. Metall. **20**, 223 (1986).
- [22] See EPAPS Document No. E-PRLTAO-103-032931 for a supplementary movie. For more information on EPAPS, see <http://www.aip.org/pubservs/epaps.html>.
- [23] A. Serra and D. J. Bacon, Philos. Mag. A **73**, 333 (1996).
- [24] A. Serra, D. J. Bacon, and R. C. Pond, Acta Mater. **47**, 1425 (1999).
- [25] R. C. Pond, D. J. Bacon, and A. Serra, Acta Mater. **47**, 1441 (1999).
- [26] B. Li and E. Ma, Philos. Mag. A **89**, 1223 (2009).